

# Detecting Anomalies in Sequential Data with Higher-order Networks

Jian Xu  
University of Notre Dame  
jxu5@nd.edu

Mandana Saebi  
University of Notre Dame  
mandana.saebi.1@nd.edu

Bruno Ribeiro  
Purdue University  
ribeiro@cs.purdue.edu

Lance M. Kaplan  
U.S. Army Research Lab  
lance.m.kaplan.civ@mail.mil

Nitesh V. Chawla  
University of Notre Dame  
nchawla@nd.edu

## ABSTRACT

A major branch of anomaly detection methods relies on dynamic networks: raw sequence data is first converted to a series of networks, then critical change points are identified in the evolving network structure. However, existing approaches use first-order networks (FONs) to represent the underlying raw data, which may lose important higher-order sequence patterns, making higher-order anomalies undetectable in subsequent analysis. We present a novel higher-order anomaly detection method that is both parameter-free and scalable, building on an improved higher-order network (HON) construction algorithm. We show the proposed higher-order anomaly detection algorithm is effective in discovering variable orders of anomalies. Our data includes a synthetic 11 billion web clickstreams and a real-world taxi trajectory data.

## CCS CONCEPTS

• **Information systems** → **Data mining**; *Social networks*; • **Theory of computation** → **Graph algorithms analysis**; • **Computing methodologies** → **Anomaly detection**;

## KEYWORDS

Anomaly detection, dynamic network, higher-order network

## 1 INTRODUCTION

Anomalies are deviation from the norm or expected behavior of a complex system. Timely and accurate detection of such anomalies is critical as they may affect the behavior or outcome of such a complex system. Moreover, the anomalies can manifest themselves as a point in time or an emerging phenomenon, presenting its own suite of challenges. The problems are more pronounced when the complex system is represented a network, given the inherent dependencies and relationships among the components (nodes) of the system. While there exists a wide range of anomaly detection methods on dynamic networks [2, 16], all of them use the first-order network (FON) to represent the underlying raw data (such as clickstreams or event sequences), which can lose important higher-order information inherent in the raw data [18, 25]. As FON is an oversimplification of higher-order dynamics, anomaly detection algorithms that rely on FONs will miss important changes in the network, thus leaving anomalies in complex systems undetected.

**Example.** Fig. 1 illustrates the challenge of detecting certain types of anomalies, using a minimal example of web clickstreams data (sequences of web page views produced by users) collected by

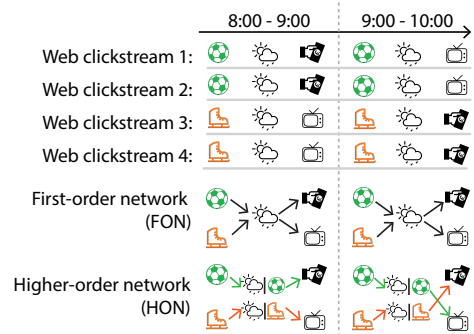


**Figure 1: Higher-order anomalies cannot be detected by network-based anomaly detection methods if FON is used.**

a local media company  $\lambda$ . Given the web clickstreams as the input to network-based anomaly detection methods, conventionally, a web traffic network is built for each time window (two one-hour windows illustrated here), with the nodes representing web pages and the edges representing total traffic between web pages. Company  $\lambda$  monitors this dynamic web traffic network; a change in the network topology indicates an anomaly in web traffic patterns. According to the original clickstreams, in the first hour, all users coming from the soccer web page to the weather page proceed to the ticket page, and all users coming from the skating page to the weather page go to TV schedules. But the flow of users is completely flipped in the next hour, possibly the weather forecast has updated with a much colder weather which is in favor of winter activities. However, despite the significant changes in user web viewing patterns, the pairwise traffic between web pages in this example remains the same, thus the FON topology shows no changes. Therefore, no matter what network-based anomaly detection method is used, if the method relies on FON, Company  $\lambda$  will not be able to detect such type of anomalies, thus failing to respond (e.g., caching pages for visits / targeted promotion of pages) to the changes in user behaviors.

**Contributions.** We systematically demonstrate why existing network-based anomaly detection methods can leave certain signals undetected, and propose to integrate HON into the anomaly detection pipeline. To achieve this objective, we also address the limitations of our prior work [25] on HON construction, namely, the dependency on multiple parameters and scalability for higher-orders. The parameter dependency can be especially limiting for anomaly detection, given the varying nature of anomalies across different complex systems. We resolve these issues with a novel

parameter-free and scalable algorithm BuildHON+. We also show that BuildHON+ can be plugged in existing anomaly detection approaches on large data with only a small overhead.

Using a large-scale synthetic clickstream data with 11 billion clicks, we show how multiple existing anomaly detection methods that depend on FON collectively fail to capture anomalous navigation behaviors beyond first order, and how BuildHON+ can solve the problem. We also demonstrate BuildHON+ on a real-world taxi trajectory data, showing its ability in amplifying higher-order anomaly signals and revealing the anomalous locations. Finally, we provide complexity analysis of BuildHON+, as well as performance analysis (running time and memory consumption) on the global ship movement data which is known to exhibit dependencies beyond fifth order. All code and data are made available online.<sup>1</sup>

## 2 RELATED WORK

**Terminology.** In literature, the term “anomaly detection” appears interchangeably with “change point detection” and “event detection”. All three terms represent a state that deviates from the “norm”, among which “anomaly” more frequently refers to a state that changes back to the norm soon, whereas a “change point” may not change back. In this paper, we refer to the more general “change point detection”, whereas anomalies that change back to the norm can be seen as two consecutive change points and can be detected along with change points.

**Anomaly detection in sequential data.** There are two directions of sequential data anomaly detection tasks. Suppose the input data has clickstreams of multiple users, one direction is to identify users with clickstreams significantly different than others (e.g., capturing hacking behaviors); this direction has been studied with sequence similarities [4, 21], sliding windows [24], Markovian methods [11, 17, 22], HMM methods [10], and so on. The other direction is to identify the time window when most users suddenly change their browsing patterns (revealing breaking news, crowd behavior changes, etc.). It is also known as “event detection”, which has been studied with sliding windows [5–7] and dynamic networks [2]. A comprehensive review is in [3]. This paper focuses on the identification of anomalous time windows rather than individual trajectories, thus relates closer with the second category.

**Anomaly detection in dynamic networks.** Unlike the task of detecting anomalous nodes and edges in a single static network (such as [1]), anomaly detection in dynamic networks [2, 3] uses multiple snapshots of networks to represent the interactions of interest (such as interacting molecules [15], elements in frames of videos [19], flow of invasive species [26], etc.), then identifies the time when the network topology shows significant changes, using network distance metrics [8, 14, 20], probability methods [13], subgraph methods like [12] and more. Nevertheless, all existing methods rely on the conventional FON; as we will show, certain types of anomalies cannot be detected with any network-based anomaly detection methods if FON is used. Rather than proposing another approach to identify the anomalous network from a series of networks, our innovation lies in the network construction step, which ensures anomalous signals are preserved in the network in the first place.

<sup>1</sup><https://github.com/xyjprc/hon>

## 3 METHODS

Our previously developed algorithm, BuildHON cannot be adapted directly to network-based anomaly detection due to (1) parameter-dependent results and (2) scalability constraints. BuildHON requires two parameters which had to be specified experimentally, depending on the data set. Furthermore, it uses an exhaustive search for extracting dependency rules and network construction, which becomes impractical for anomaly detection. We overcome these limitations through a higher order anomaly detection framework, including improved HON construction algorithm, BuildHON+, which makes it practical to use HON for anomaly detection tasks.

### 3.1 Higher-order Anomaly Detection

In this subsection, we review the network-based anomaly detection framework, and demonstrate why HON should be used.

**Definition.** The procedure of a network-based anomaly detection method takes the sequential data,  $\mathcal{S} = [S_1, S_2, \dots, S_T]$  which is divided into  $T$  time windows  $t \in [1, T]$  as the input. In each time window, the sequential data is represented as a network, i.e.,  $S_i \rightarrow G_i$ , yielding a dynamic network  $\mathcal{G} = [G_1, G_2, \dots, G_T]$  composed of the sequence of networks. The dynamic network  $\mathcal{G}$  is then used to find the change point(s)  $t \in [1, T]$  when  $G_t$  is significantly different from  $G_{t-1}$ . The difference between networks in neighboring time intervals, i.e.,  $d_t = \mathcal{D}(G_{t-1}, G_t)$ , can be quantified by network distance metrics  $\mathcal{D}$  (e.g., [8, 14, 20]). Then the problem of anomaly detection on networks reduces to anomaly detection in the time series of  $[d_2, d_3, \dots, d_T]$ . Next, to determine if the network difference  $d_t$  is significantly high, straightforwardly, if  $d_t$  is larger than a fixed threshold  $\Delta$ ,  $G_t$  is anomalously different than  $G_{t-1}$ . Another more robust way is to establish the norm of network differences by computing the running average and standard deviation of network differences in the last  $k$  time intervals, the null hypothesis being  $d_t$  not significantly large; if  $d_t$  deviates from the running average by one or more standard deviations, the null hypothesis is rejected and time  $t$  is considered a change point.

Existing network-based anomaly detection methods mostly differ at the network distance calculation step. However, for the  $S_i \rightarrow G_i$  step, i.e., where raw sequential data is represented as networks, existing methods all use the first-order network (FON) as  $G$  to represent the underlying sequential data  $S$ , by counting the occurrences of pairs (bigrams) as edge weights in the network. Here for the first time, we propose to use the higher-order network (HON) that selectively embeds  $n$ -grams for the  $S_i \rightarrow G_i$  step. HON keeps all structures of FON, and when higher-order dependencies exist in the raw sequential data, it splits a node into multiple nodes representing previous steps [25]. We show that certain types of anomalies will remain undetected for all existing network-based anomaly detection methods using FON, but can be revealed by using HON.

**Example.** Fig. 2 illustrates a side-by-side comparison of FON and HON in the network representation step. Suppose there are four user sessions in the web clickstream data. In time window I, users at web page  $c$  randomly navigate to  $d$  or  $e$ , regardless if the users came to page  $c$  from  $a$  or  $b$ . In this time window, HON is identical to FON and there are no higher-order dependencies. In time window II, the clickstreams are randomly shuffled, and the

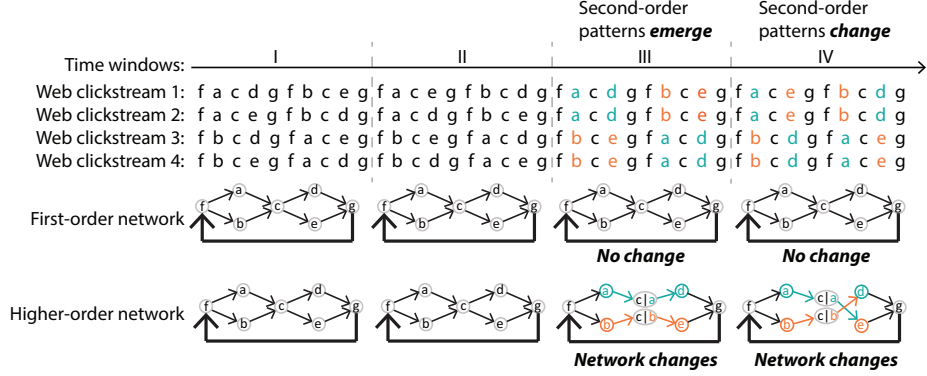


Figure 2: Comparing anomaly detection based on the first-order dynamic network and the higher-order dynamic network.

pairwise traffic between pages  $a, b, c, d, e$  remains the same as time window I. Neither FON nor HON shows changes.

In time window III, second-order patterns *emerge*: all users that had navigated from  $a$  to  $c$  go to  $d$ , and all users from  $b$  to  $c$  go to  $e$ . Since the aggregated traffic from  $c$  to  $d$  and  $e$  remains the same, the FON remains *exactly the same*, missing this newly emerged pattern. In contrast, HON uses additional higher-order nodes and edges to capture higher-order dependencies: node  $c$  is now splitted into a new node  $c|a$  (representing  $c$  given the last step being  $a$ ) and node  $c|b$  (representing  $c$  given the last step being  $b$ ). The path  $a \rightarrow c \rightarrow d$  now becomes  $a \rightarrow c|a \rightarrow d$ ; the edge  $c \rightarrow e$  rewired similarly. Therefore, the emergence of the second-order pattern in the raw data is reflected by the non-trivial changes in the topology of HON. If we use the weight distance [20] defined as

$$\mathcal{D}(G, H) = |E_G \cup E_H|^{-1} \sum_{u, v \in V} \frac{|w_E^G(u, v) - w_E^H(u, v)|}{\max\{w_E^G(u, v), w_E^H(u, v)\}} \quad (1)$$

with  $w$  being the edge weights and  $|E|$  being the total number of edges, due to the complete changes in four out of the nine edges on HON, the network distance  $\mathcal{D}(G_2, G_3) = 0.44 > 0$ , successfully captures this *higher-order anomaly* (a significant change in higher-order navigation patterns).

In time window IV, the second-order browsing pattern *changes*: all users that navigated from web page  $a$  to  $c$  now visit page  $e$  instead of  $d$ , and all from  $b$  to  $c$  now visit  $d$  instead of  $e$ . Since the pairwise clickstream traffic from  $c$  to  $d$  and  $e$  remains the same, FON remains the same. However, HON captures the changes with two edge rewirings: now  $c|a \rightarrow e$  and  $c|b \rightarrow d$ , resulting in  $\mathcal{D}(G_3, G_4) = 0.22 > 0$ .

In brief, FON is an oversimplification of sequential data produced by complex systems, and conventional network-based anomaly detection methods that use FON may fail to capture the emergence and changes of higher-order navigation patterns. If HON is used instead, without changes to distance metrics, existing methods can capture these previously ignored anomalies.

### 3.2 BuildHON+: Building HON from Big Data

Anomaly detection algorithms should have only **one** parameter: the *detection threshold*. Unfortunately, as is, the existing HON construction algorithm BuildHON [25] is not suited for anomaly detection.

It needs two parameters in addition to the detection threshold: a *MaxOrder* parameter which governs how many orders of dependencies the algorithm will consider in HON, and a *MinSupport* parameter that discards infrequent observations. As a result, anomaly detection using BuildHON is susceptible to parameters irrelevant to the detection threshold. BuildHON also does not scale to large networks, precisely when anomaly detection is most needed due to the complexity of the data and the inability to properly visualize it.

Here we introduce BuildHON+, a parameter-free algorithm that constructs HON from big data sets. BuildHON+ is the first practical approach that preserves higher-order signals in the network representation step ( $S_i \rightarrow G_i$ ) which is essential for anomaly detection. Using BuildHON+, our anomaly detection has only one parameter: the *detection threshold*. The difference between BuildHON and BuildHON+ is similar to the difference between pruning and early stopping in decision trees. BuildHON first builds an HON of all orders from first order to *MaxOrder* and then selects branches showing significant higher-order dependencies. BuildHON+ reduces the search space beforehand by checking in each step if increasing the order may produce significant dependencies.

**3.2.1 BuildHON.** The core of BuildHON is the dependency rule extraction step, which answers whether higher-order dependencies exist in the raw sequential data, and how high the orders are. The dependency rules extracted are then converted to higher-order nodes and edges as the building blocks of HON. Rather than deriving a fixed order of dependency for the whole network, the method allows for variable orders of dependencies for more compact representation. Fig. 3 illustrates the dependency rule extraction step. BuildHON first counts the observed n-grams in the raw data (step ①), then compute probability distributions for the next steps given the current and previous steps (step ②). Finally test if knowing one more previous step significantly changes the distribution for the next step – if so, higher-order dependency exists for the path (step ④); this procedure (“rule growing”) is iterated recursively until a pre-defined *MaxOrder* (shown here *MaxOrder* = 3). In this example, the probability distribution of the next steps from  $C$  changes significantly if the previous step (coming to  $C$  from  $A$  or  $B$ ) is known (step ④), but knowing more previous steps (coming to  $C$  from  $E \rightarrow A$

or  $D \rightarrow B$ ) does not make a difference (step ⑤); therefore, paths  $C|A \rightarrow D$  and  $C|A \rightarrow E$  demonstrate second-order dependencies.

Formally, the “rule growing” process works as follows: for each path (n-gram)  $\mathcal{S} = [S_{t-k}, S_{t-(k-1)}, \dots, S_t]$  of order  $k$ , starting from the first order  $k = 1$ , assume  $k$  is the true order of dependency, which  $\mathcal{S}$  has the distribution  $D$  for the next step. Then extend  $\mathcal{S}$  to  $\mathcal{S}_{ext} = [S_{t-(k+1)}, S_{t-k}, S_{t-(k-1)}, \dots, S_t]$  by adding one more previous step;  $\mathcal{S}_{ext}$  has order  $k_{ext} = k + 1$  and distribution  $D_{ext}$ . Next, test if  $D_{ext}$  is significantly different than that of  $D$  using Kullback-Leibler divergence [9] as  $\mathcal{D}_{KL}(D_{ext}||D)$ , and compare with a dynamic threshold  $\delta$  – if the divergence is larger than  $\delta$ , order  $k + 1$  is assumed instead of  $k$  for the path  $\mathcal{S}_{ext}$ . The dynamic threshold  $\delta$  is defined as  $\delta = \frac{k_{ext}}{\log_2(1+Support_{\mathcal{S}_{ext}})}$ , so that lower orders are preferred than higher orders, unless higher order paths have sufficient support (number of observations). The whole process is iterated recursively until *MaxOrder*.

**3.2.2 Eliminating all parameters.** The reason for having the *MaxOrder* and *MinSupport* parameters in BuildHON is to set a hard stop for the rule growing process, otherwise it will iterate indefinitely and keep extending  $\mathcal{S}$ . Here we show how we can pre-determine if extending  $\mathcal{S}$  will not produce significantly different distributions.

LEMMA 3.1. *The significance threshold  $\delta = \frac{k_{ext}}{\log_2(1+Support_{\mathcal{S}_{ext}})}$  increases monotonically in rule growing when expanding  $\mathcal{S}$  to  $\mathcal{S}_{ext}$ .*

PROOF. On the numerator, the order  $k_{ext}$  of the extended sequence  $\mathcal{S}_{ext}$  increases monotonically with the inclusion of more previous steps. Meanwhile, every observations of  $[S_{t-(k+1)}, S_{t-k}, \dots, S_{t-1}, S_t]$  in the raw data can find a corresponding observation of  $[S_{t-k}, \dots, S_{t-1}, S_t]$ , but not the other way around. Therefore, the support of  $\mathcal{S}_{ext}$ ,  $Support_{\mathcal{S}_{ext}} \leq Support_{\mathcal{S}}$  of the lower order  $k = k_{ext} - 1$ . As a result, the denominator decreases monotonically with the rule growing process.  $\square$

Given the next step distribution  $D = [P_1, P_2, \dots, P_N]$  of sequence  $\mathcal{S}$ , we can derive an upper-bound of possible divergence:

$$\begin{aligned} & \max(\mathcal{D}_{KL}(D_{ext}||D)) \\ &= \max\left(\sum_{i \in D} P_{ext}(i) \times \log_2 \frac{P_{ext}(i)}{P(i)}\right) \\ &\leq 1 \times \log_2 \frac{1}{\min(P(i))} + 0 + 0 + \dots \\ &= -\log_2(\min(P(i))) \end{aligned} \quad (2)$$

The equal sign (maximum possible divergence) is taken iff the least likely option for the next step  $P(i)$  in  $\mathcal{S}$  becomes the most likely option  $P_{ext}(i) = 1$  in  $\mathcal{S}_{ext}$ , and all other options have  $P = 0$ . Therefore, we can test if  $-\log_2(\min(P_{Distr}(i))) < \delta$  holds during the rule growing process; if it holds, then further increasing the order (adding more previous steps) will not produce significantly different distributions, so we can stop the rule growing process and take the last known  $k$  as the true order of dependency. An advantage of this proposed parameter-free approach is that rather than terminating the rule growing process prematurely by the *MaxOrder* threshold, the algorithm can now extract *arbitrarily high order of dependency*.

**3.2.3 Scalability for Higher-orders.** BuildHON builds all observations and distributions up to *MaxOrder* ahead of the rule growing process (Fig. 3 left). This procedure becomes prohibitively expensive for big data and data with high orders of dependencies: to extract sparse tenth order dependencies, BuildHON needs to enumerate n-grams from first order to tenth order and compare probability distributions, which already exceeds a personal computer’s capacity using a typical real-world data set (see Section 4.3).

Our contribution, BuildHON+, uses *lazy construction* of observations and distributions which has a much smaller search space, and can easily scale to arbitrarily high order of dependency. Specifically, we do not count the occurrences of n-grams, nor calculate the distribution of the next steps, until the rule growing step explicitly asks for such information.

**Example.** BuildHON+ first builds all first-order observations and distributions (Fig. 3 right step ①–③). Given that  $A \rightarrow C$ ,  $B \rightarrow C$ ,  $D \rightarrow B$ ,  $E \rightarrow A$  all have single deterministic options for the next step with  $P = 1$ , according to  $-\log_2(\min(P_{Distr}(i))) = 0 < \delta$ , BuildHON+ knows no higher-order dependencies can possibly exist by extending these bigrams (step ④). Only the two paths  $C \rightarrow D$  and  $C \rightarrow E$  will be extended; since the corresponding second-order observations and distributions are not known yet, BuildHON+ *selectively* derives the necessary information from the raw data (Fig. 3 right step ⑤–⑦), and finds that the second-order distributions show significant changes. At this point, both  $C|A \rightarrow D$  and  $C|B \rightarrow E$  have single deterministic options for the next step, so again, BuildHON+ determines no dependencies beyond second order can exist (step ⑧), so the rule growing procedure stops, without the need for further generation and comparison of distributions.

The challenge is how to count the n-gram of interest on demand – seemingly every on-demand construction requires a traversal of the raw sequential data with complexity of  $\Theta(L)$ . However, given the following knowledge:

LEMMA 3.2. *All observations of the sequence  $[S_{t-k-1}, S_{t-k}, \dots, S_{t-1}, S_t]$  can be found exactly at the current and one preceding locations of all observations of sequence  $[S_{t-k}, \dots, S_{t-1}, S_t]$  in the raw data.*

Instead of traversing the raw data, we use an *indexing cache* to store the locations of known observations, then use that to narrow down higher-order n-gram look-ups. As illustrated in Fig. 3, if we cache the locations of  $C \rightarrow D$  and  $C \rightarrow E$  in the raw sequential data, then  $C|A \rightarrow D$  and  $C|B \rightarrow E$  can be found at the same locations.

During the rule growing process, if  $\mathcal{S}_{ext}$  has not been observed, *recursively* check if the lower-order observation is in the indexing cache, and use those cached indexes to perform fast lookup in the raw data. New observations from  $\mathcal{S}_{ext}$  are then added to the indexing cache. This procedure guarantees the identification of observations of the previously unseen  $\mathcal{S}_{ext}$ , and the lookup time for each observation is  $\Theta(1)$  when the indexing cache is implemented with hash tables.

**Complexity analysis.** We formally analyze the computational complexity of BuildHON. Suppose the size of raw sequential data is  $L$ , all first order observations (bigrams) take  $\Theta(2L)$  space, second order observations (trigrams) take  $\Theta(3L)$  space, and so on; building observations and distributions up to  $k^{th}$  order takes  $\Theta(2L +$

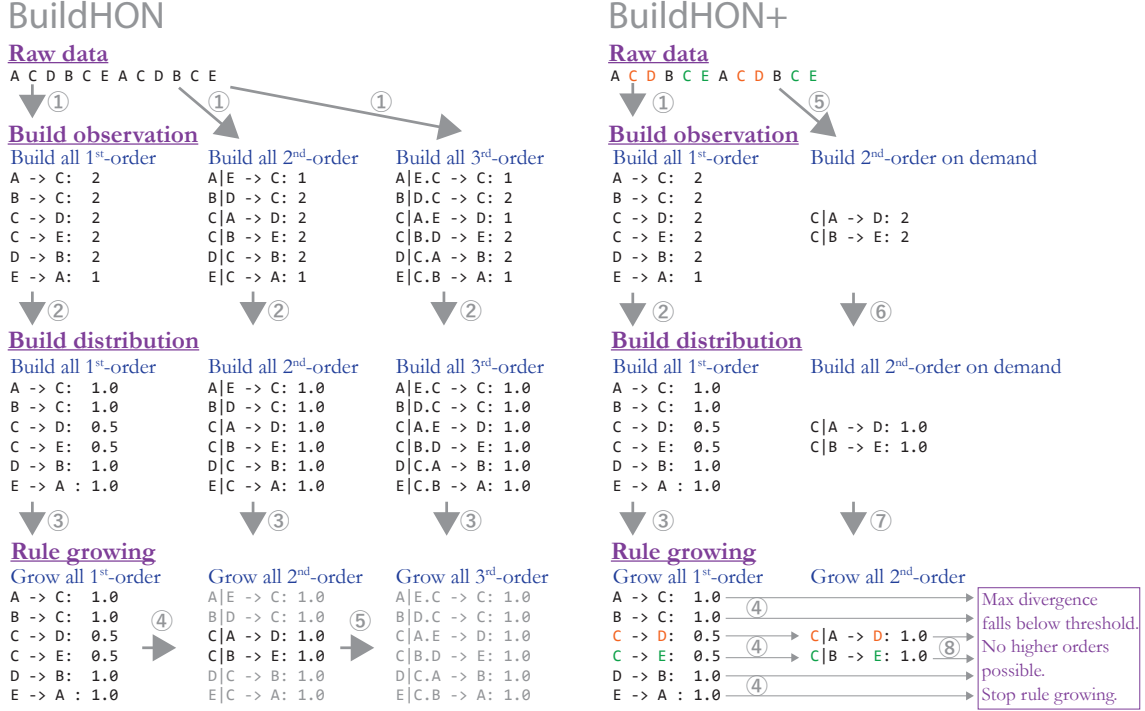


Figure 3: Comparison of the *active* observation construction in BuildHON (left) and the *lazy* observation construction in BuildHON+ (right, with a much smaller search space). Circled numbers represent the order of execution.

$3L + 4L + \dots + (k + 1)L = \Theta(k^2L)$  storage. Suppose  $N$  is the number of unique entities in the raw data, the time complexity of the algorithm is  $\Theta(Nk^2L)$ : all observations will be traversed at least once; testing if adding a previous step significantly changes the probability distribution of the next step takes up to  $\Theta(N)$  time (if Kullback-Leibler divergence [9] is used).

On BuildHON+, space complexity is  $\Theta(2R_1 + 3R_2 + \dots)$  (including observations, distributions, and the indexing cache), where  $R_k$  is the *actual* number of higher-order dependency rules for order  $k$ . Since  $R_k \leq L$ , and in practice, when  $k \gg 2$ ,  $R_k \ll L$  (higher-order rules are usually sparse), the overall space complexity of BuildHON+ is significantly smaller than that of BuildHON (which is  $\Theta(k^2L)$ ). The same applies to time complexity: while BuildHON has  $\Theta(Nk^2L)$ , BuildHON+ has  $\Theta(N(2R_1 + 3R_2 + \dots))$ . A side-by-side comparison between BuildHON and BuildHON+ in running time and memory consumption on a real-world data set is provided in Section 4.3.

## 4 RESULTS

In this section, we first construct a large-scale synthetic clickstream data with 11 billion movements and variable orders of dependencies, and show that five existing anomaly detection methods based on FON collectively fail to capture anomalous navigation behaviors beyond first order, while using our framework, all methods show significant improvements. We also demonstrate HON on a real-world taxi trajectory data, showing its ability in amplifying higher-order anomaly signals and revealing the exact location of anomalies. Note that we use the proposed BuildHON+ algorithm to construct

HON for all following experiments, except for the last step where we compare with BuildHON in terms of running time and memory consumption on real-world data.

### 4.1 Large-scale Synthetic Web Clickstreams

We first use the synthetic web clickstream data to test the effectiveness of the HON-based anomaly detection framework. With synthetic data, we know exactly when, where, and what types of anomalies exist. To begin with, we assume there are 100,000 users navigating through 100 web pages which are organized as a  $10 \times 10$  grid (for convenient illustration) and numbered from 00 to 99. Every page has two out-links to the neighboring pages, one pointing right and one pointing down, with wrapping (a rightmost page can point to the leftmost page in the same row, and a bottom page can point to the top page in the same column). At each time stamp, every user clicks through 100 pages by moving right or moving down, resulting in 10,000,000 records per time stamp.

Our goal is to synthesize input sequences with variable orders of user navigating patterns. We start from the basic case where all users navigate randomly, then gradually add or change first-order and higher-order navigation rules, and see if the proposed method can successfully identify these anomalies. For each of the following 11 cases, we maintain the user navigation behavior for 100 time windows. In total, we generate 11,000,000,000 clicks for the subsequent anomaly detection task. The full process to synthesize the input trajectories is illustrated in Fig. 4.

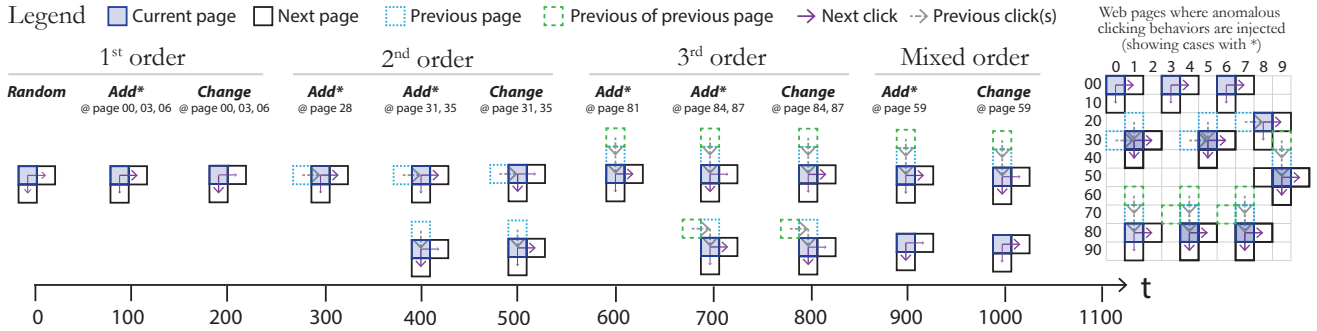


Figure 4: Synthetic web clickstream data: variable orders of user browsing patterns on 100 web pages as a 10x10 grid.

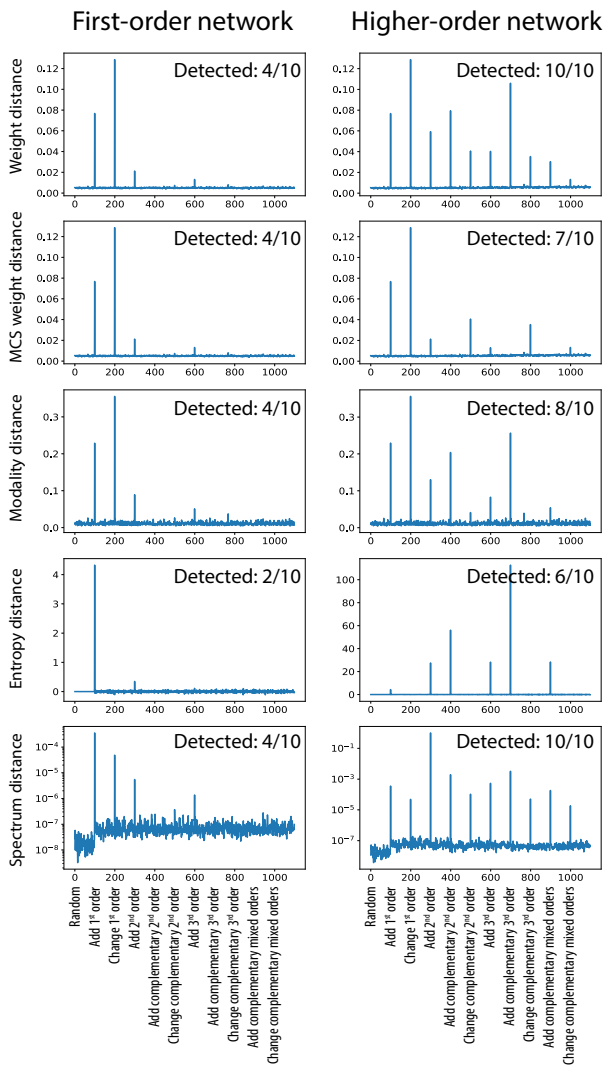


Figure 5: Methods that use FON collectively fail to capture anomalous navigation behaviors beyond first order no matter what distance metric is used, but all show signals when HON is used instead.

**Initial random movement case.** At  $t = [0, 99]$ , each user has 50% chance of navigating to the page on the right and 50% chance of navigating down in each click.

**Emergence of first-order dependency.** At  $t = [100, 199]$ , we impose the following first-order rule of movement: all users landing on page 00, 03 and 06 will have 90% chance of navigating to the page on the right in the next step, and 10% chance of moving down. This new rule incurs a significant change of first-order clickstream traffic at  $t = 100$  between pages 00–01, 00–10, 03–04, 03–13, 06–07 and 06–16. The locations of these dependency rules are highlighted on the right of Fig. 4.

**Change of first-order dependency.** At  $t = [200, 299]$ , we change the existing first-order movement rules: all users coming to page 00, 03 and 06 will now have 90% chance of moving down in the next step, and 10% chance of moving right. Pairwise clickstream traffic changes again at  $t = 200$ .

**Emergence of second-order dependency.** At  $t = [300, 399]$ , we keep the previous first-order rules, and impose a new second-order rule: all users coming from page 27 to 28 will have 90% chance of moving to the right in the next step, and 10% chance of moving down. This change at  $t = 300$  not only introduces new higher-order dependencies, but also slightly influences first-order traffic (traffic of  $27 \rightarrow 28 \rightarrow 29/38$  changes from 1:1 to 7:3).

**Emergence of complementary second-order dependencies.** At  $t = [400, 499]$ , we impose a pair of new second-order rules: (1) all users coming from page 30 to 31 (and 34 to 35) will have 90% chance of moving to the right in the next step, and 10% chance of moving down; (2) all users coming from page 21 to 31 (and 25 to 35) will have 90% chance of moving down, and 10% chance of moving right. The combined effect of these two new complementary second-order dependencies at  $t = 400$  is that the first-order clickstream traffic from page 31 and 35 remains unchanged.

**Change of complementary second-order dependencies.** At  $t = [500, 599]$ , we flip the rules for the complementary second-order dependencies: (1) all users coming from page 30 to 31 (and 34 to 35) will have 90% chance of moving down, and 10% chance of moving right; (2) all users coming from page 21 to 31 (and 25 to 35) will have 90% chance of moving right, and 10% chance of moving down. At  $t = 500$  the first-order clickstream traffic from cell 31 and 35 still remains unchanged.

**Emergence of third-order dependency.** At  $t = [600, 699]$ , we impose a new third-order rule: all users coming from cell 61

through 71 to 81 will have 90% chance of moving to the right in the next step, and 10% chance of moving down. This introduction of third-order dependency at  $t = 600$  also slightly influences the first-order traffic (from 1:1 to 3:2).

**Emergence of complementary third-order dependencies.** At  $t = [700, 799]$ , we impose a pair of new third-order rules: (1) all users coming from page 64 through 74 to 84 (and 67 through 77 to 87) will have 90% chance of moving to the right in the next step, and 10% chance of moving down; (2) all users coming from 73 through 74 to 84 (and 76 through 77 to 87) will have 90% chance of moving down, and 10% chance of moving right. Here at  $t = 700$  first-order traffic does not change when these two complementary third-order dependencies are introduced together.

**Change of complementary third-order dependencies.** At  $t = [800, 899]$ , we flip the rules for the complementary third-order dependencies. First-order traffic at  $t = 800$  again remains unchanged.

**Emergence of complementary mixed-order dependency.** At  $t = [900, 999]$ , we impose a new third-order rule and a first-order rule: (1) all users coming from page 39 through 49 to 59 will have 90% chance of moving to the right in the next step, and 10% chance of moving down; (2) all users at cell 59 will have 11/30 chance of moving right and 19/30 chance of moving down. At  $t = 900$  first-order traffic does not change, because the influence of the new third-order rule on pairwise traffic is canceled by the new first-order rule.

**Change of complementary mixed-order dependency.** At  $t = [1000, 1099]$ , we flip the rules for the mixed-order dependencies. First-order traffic at  $t = 1000$  remains unchanged.

**4.1.1 Distance Metrics.** As for the network distance metric  $\mathcal{D}$ , we evaluate five graph distance measures here, the first one being the **weight distance** introduced earlier (Equation 1).

The second is **maximum common subgraph** (MCS) distance, defined similar to the weight distance in Equation 1 but operates on the maximum common subgraph [20]:

$$\mathcal{D}(G, H) = |E_G \cap E_H|^{-1} \sum_{u, v \in V} \frac{|w_E^G(u, v) - w_E^H(u, v)|}{\max\{w_E^G(u, v), w_E^H(u, v)\}} \quad (3)$$

The third is **modality** [8]:

$$\mathcal{D}(G, H) = \|\pi(G) - \pi(H)\| \quad (4)$$

where  $\pi(G)$  and  $\pi(H)$  are the Perron vectors of graphs  $G$  and  $H$ , respectively.

Fourth is the **entropy graph distance** [14]:

$$\mathcal{D}(G, H) = E(G) - E(H) \quad (5)$$

where  $E(*)$  is the entropy measure of the edges:

$$E(*) = \sum_{e \in E_*} \tilde{W}_*^e - \sum_{e \in E_*} \ln \tilde{W}_*^e \quad (6)$$

and:

$$\tilde{W}_*^e = \frac{W_*^e}{\sum_{e \in E_*} W_*^e} \quad (7)$$

is the normalized weight for edge  $e$ .

Fifth is the **spectral distance** [14]:

$$\mathcal{D}(G, H) = \sqrt{\frac{\sum_{i=1}^k (\lambda_i - \mu_i)^2}{\min(\sum_{i=1}^k \lambda_i^2, \sum_{i=1}^k \mu_i^2)}} \quad (8)$$

where  $\lambda_i$  and  $\mu_i$  represent the eigenvalues of the Laplacian matrix for graph  $G$  and  $H$ , respectively.

**4.1.2 Anomaly Detection Results.** For all five distance metrics, we present a side-by-side comparison between anomaly detection results using FON and HON in Fig. 5. The Y-axis shows the graph distances between neighboring time windows; given that we have injected 10 anomalous movement patterns at  $t = [100, 200, \dots, 1000]$ , we should expect to see 10 “spikes” in graph distances.

Methods using FON can detect at most 4 out of the 10 anomalies: the addition and changes in first-order movement patterns ( $t = 100, t = 200$ ), the addition of second-order ( $t = 300, t = 600$ ), and the addition of third-order ( $t = 600$ ) movement patterns. Because the latter two cases also slightly change the first-order traffic, FON does reflect the changes, but the spikes incurred are not as significant as when changes are made directly to first-order rules. For the other six cases, all five distance metrics appear as if there are no anomalies, as long as they rely on FON topology.

In contrast, methods using HON (1) capture all first-order anomalies ( $t = 100, t = 200$ ); (2) show stronger signals for the addition of second-order and third-order rules ( $t = 300, t = 600$ ) because not only the first-order traffic is changed but BuildHON+ also creates additional higher-order nodes and edges for higher-order dependencies; (3) capture the six additional cases where higher-order movement patterns are changed but first-order clickstream traffic remain the same. Here the topological changes of HON are best reflected with weight distance and spectrum distance (detecting 10/10 anomalies); MCS weight method misses the addition of higher-order nodes and edges ( $t = 400, 700, 900$ ) because those topological changes are excluded from common subgraphs; entropy method misses changes in edge weights ( $t = 200, 500, 800, 1000$ ), also because by definition a swap in edge weights does not change a graph’s entropy. Nevertheless, all these distance metrics are able to identify more types of anomalous signals simply by using HON instead of FON, with no changes to these distance metrics. In other words, BuildHON+ can be plugged in to existing graph-based anomaly detection methods directly, and extend their ability in detecting higher-order anomalies.

## 4.2 Real-world Porto Taxi Data

We use the ECML/PKDD 2015 challenge data<sup>2</sup>, which contains one year (Jul. 1, 2013 to Jun. 30, 2014) of all the 442 taxi GPS trajectories in Porto, Portugal. The coordinates of each taxi was collected at every 15 seconds. To discretize the geolocation data into points of interests that are representative of population density, we map all coordinates to the nearest 41 police stations (Fig. 7(a)). We take every week as a single time window, yielding 52 time windows, each containing 442 trajectories of points of interest. In each week, the trajectories (after removing repetitive points of interest) are used to construct the FON and HON traffic networks of the week.

<sup>2</sup><http://www.geolink.pt/ecmlpkdd2015-challenge/dataset.html>

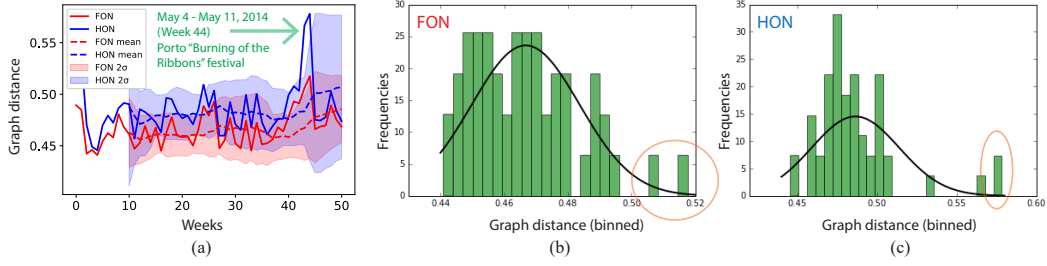


Figure 6: (a) Anomaly detection results on the dynamic network of FON and HON. (b) and (c) HON amplifies the anomalous traffic patterns.

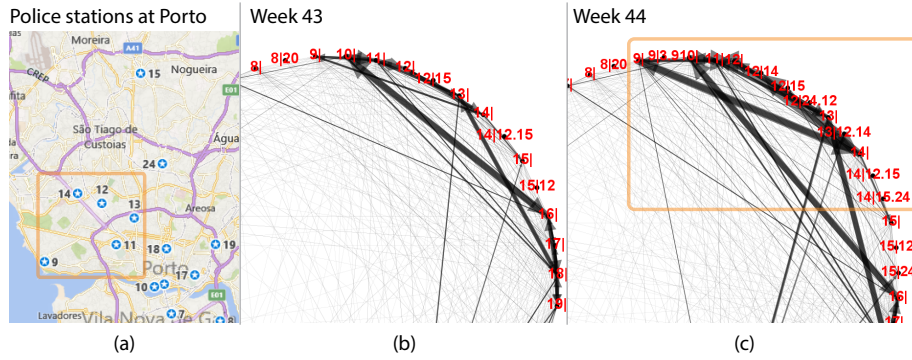


Figure 7: (a) Labeling of police stations in urban areas of Porto. (b) and (c) the emergence of higher-order traffic patterns in Week 44 (“Burning of the Ribbons” festival) captured by HON, corresponding to the highlighted region in (a).

4.2.1 *Observations with FON and HON.* Given the 52 networks for both FON and HON, we compute the graph distances (using weight distance) for neighboring time windows, as in Fig. 6(a). We also compute the running average and standard deviation using the graph distances in previous 10 weeks, with the null hypothesis as “the network is not significantly different if the graph distance does not deviate more than  $2\sigma$  from the mean”. While the trend of HON resembles that of FON, the graph distances in Week 44 are particularly more significant in HON than that in FON. Such differences are also indicated in the histograms of graph distances in Fig. 6(b) and (c), where the orange circles highlight the same anomalous signals, which is more significant on HON than on FON.

We focus on the case of Week 44 to understand why HON produces stronger signal than FON in this time window. We notice that Porto’s second most important festival, “Burning of the Ribbons”, lasts from May 4 to May 11 in 2014 and falls within Week 44 of our study. The festival involves parades, road closures, and is popular among tourists, which could be the underlying reason to the changes in taxis’ movement patterns. After plotting the traffic HON of Week 43 and Week 44 in Fig. 7, we notice that multiple higher-order nodes and edges emerge in Week 44, indicating the emergence of higher-order traffic patterns. The newly emerged higher-order patterns correspond to police stations labeled from 9 to 14, which is where the event’s main venue (Queim-Årdromo in the City Park) and participating universities are located.<sup>3</sup> Due to the

<sup>3</sup><http://www.maiahoje.pt/noticias/ler-noticia.php?noticia=577>

changes in additional nodes and edges in HON compared to FON (which only captures the aggregated first-order traffic changes), the anomalous signals are amplified on HON.

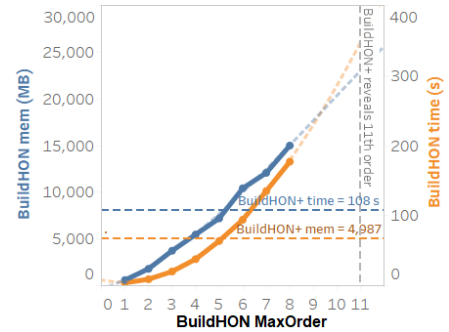


Figure 8: Given the same data [25], BuildHON+ extracts up to 11<sup>th</sup> order in 1/3 run-time and 1/5 memory of BuildHON.

### 4.3 Performance improvement of BuildHON+

To highlight the scalability advantage of BuildHON+, instead of the taxi data or the synthetic data (which demonstrates up to third order of dependency), we use the same shipping trajectories data as used in the HON paper [25]. This data was shown to demonstrate dependencies of more than the fifth order due to ships’ cyclic

movement patterns. It consists of 3,415,577 voyages made by 65,591 ships between May 1<sup>st</sup>, 2012 and April 30<sup>th</sup>, 2013.

For fair comparison, we use the Python implementation for both BuildHON+ and BuildHON. Both implementations run single-threaded on the same laptop (Intel i7-6600U @ 2.60GHz, 16GB RAM, SSD). BuildHON+ is parameter-free (no limit to the maximum order, optional `MinSupport = 1`) and does not require further configuration. We set `MinSupport = 1` for BuildHON, and gradually increase `MaxOrder` from the first order. BuildHON+ was able to find up to 11<sup>th</sup> order within 2 minutes, with a peak memory usage less than 5GB, as the reference lines displayed in Fig. 8. In comparison, BuildHON already exceeds the running time and memory consumption of BuildHON+ at 6<sup>th</sup> order, reaches the physical memory limit (16GB) of a high-end laptop at 8<sup>th</sup> order, and would need about 22 GB memory and 6 minutes (3x time and 5x memory than BuildHON+) to achieve the same results as BuildHON+ can.

## 5 DISCUSSION

This paper presents a higher-order network (HON) approach for anomaly detection, which is capable of detecting higher-order anomalies in sequences. In this work, we focused on two key elements: efficiency, and accuracy. In terms of accuracy, we show that higher-order anomalies can remain completely undetected using all existing anomaly detection methods that rely on the first-order network (FON). On the efficiency side, we show that despite the advantages of HON, our existing HON construction algorithm is not suitable for anomaly detection due to the extra parameters and poor scalability for big data. We introduce BuildHON+, a parameter-free algorithm that constructs HON from big data sets.

We show with a large-scale synthetic web clickstream data how multiple existing anomaly detection methods that depend on FON fail to capture higher-order anomalous navigation behaviors; we further show how HON can be plugged in to existing methods to enable the detection of various orders of anomalies. We also demonstrate HON on a real-world taxi trajectory data, showing its ability in amplifying higher-order anomaly signals and locating anomalies. Finally, we provide complexity analysis of BuildHON+, as well as running time and memory consumption benchmarking results, which demonstrates how one can improve existing anomaly detection approaches using BuildHON+ on large data sets with a small overhead.

There are multiple directions for future improvements. First, the proposed method generalizes beyond the web to the physical world. With soccer ball-passing data, our method may be used to detect the changes in strategies. With signature data, our method may also serve as an indicator of fraud detection. For terrorist activities or network hacking records, our method can help identify attacks and higher-order anomalies. Second, while we showed various graph distance metrics, one direction is to apply structure-based metrics [2] that factor in changes of clustering or ranking results and local properties such as motifs on the network – all of these are directly compatible with BuildHON+. Finally, it would be of practical importance to integrate higher order anomaly detection into visualization frameworks such as HoNVIs [23].

## REFERENCES

- [1] Leman Akoglu, Mary McGlohon, and Christos Faloutsos. 2010. Oddball: Spotting anomalies in weighted graphs. *Advances in Knowledge Discovery and Data Mining* (2010), 410–421.
- [2] Leman Akoglu, Hanghang Tong, and Danai Koutra. 2015. Graph based anomaly detection and description: a survey. *Data Mining and Knowledge Discovery* 29, 3 (2015), 626–688.
- [3] Varun Chandola, Arindam Banerjee, and Vipin Kumar. 2012. Anomaly detection for discrete sequences: A survey. *IEEE Transactions on Knowledge and Data Engineering* 24, 5 (2012), 823–839.
- [4] Varun Chandola, Varun Mithal, and Vipin Kumar. 2008. Comparative evaluation of anomaly detection techniques for sequence data. In *Eighth IEEE International Conference on Data Mining*. IEEE, 743–748.
- [5] Eamonn Keogh, Jessica Lin, and Ada Fu. 2005. Hot sax: Efficiently finding the most unusual time series subsequence. In *Fifth IEEE International Conference on Data Mining*. IEEE, 8–pp.
- [6] Eamonn Keogh, Jessica Lin, Sang-Hee Lee, and Helga Van Herle. 2007. Finding the most unusual time series subsequence: algorithms and applications. *Knowledge and Information Systems* 11, 1 (2007), 1–27.
- [7] Eamonn Keogh, Stefano Lonardi, and Chotirat Ann Ratanamahatana. 2004. Towards parameter-free data mining. In *Proceedings of the tenth ACM SIGKDD international conference on Knowledge discovery and data mining*. ACM, 206–215.
- [8] M Kraetzl and WD Wallis. 2006. Modality distance between graphs. *Utilitas Mathematica* 69 (2006), 97–102.
- [9] Solomon Kullback and Richard A Leibler. 1951. On information and sufficiency. *The annals of mathematical statistics* 22, 1 (1951), 79–86.
- [10] Terran Lane. 1999. Hidden markov models for human/computer interface modeling. In *Proceedings of the IJCAI-99 Workshop on Learning about Users*. Citeseer, 35–44.
- [11] Christoph C Michael and Anup Ghosh. 2000. Two state-based approaches to program-based anomaly detection. In *Computer Security Applications, 2000. ACSAC'00. 16th Annual Conference*. IEEE, 21–30.
- [12] Misael Mongiovi, Petko Bogdanov, Razvan Ranca, Evangelos E Papalexakis, Christos Faloutsos, and Ambuj K Singh. 2013. NetSpot: Spotting significant anomalous regions on dynamic networks. In *Proceedings of the 2013 SIAM International Conference on Data Mining*. SIAM, 28–36.
- [13] Leto Peel and Aaron Clauset. 2015. Detecting Change Points in the Large-Scale Structure of Evolving Networks.. In *AAAI*. 2914–2920.
- [14] Brandon Pincombe. 2005. Anomaly detection in time series of graphs using arma processes. *Asor Bulletin* 24, 4 (2005), 2.
- [15] Arvind Ramanathan, Pratul K Agarwal, Maria Kurnikova, and Christopher J Langmead. 2010. An online approach for mining collective behaviors from molecular dynamics simulations. *Journal of Computational Biology* 17, 3 (2010), 309–324.
- [16] Stephen Ranshous, Shitian Shen, Danai Koutra, Steve Harenberg, Christos Faloutsos, and Nagiza F Samatova. 2015. Anomaly detection in dynamic networks: a survey. *Wiley Interdisciplinary Reviews: Computational Statistics* 7, 3 (2015), 223–247.
- [17] Dana Ron, Yoram Singer, and Naftali Tishby. 1994. Learning probabilistic automata with variable memory length. In *Proceedings of the seventh annual conference on Computational learning theory*. ACM, 35–46.
- [18] Martin Rosvall, Alcides V Esquivel, Andrea Lancichinetti, Jevin D West, and Renaud Lambiotte. 2014. Memory in network flows and its effects on spreading dynamics and community detection. *Nature communications* 5 (2014).
- [19] Venkatesh Saligrama and Zhu Chen. 2012. Video anomaly detection based on local statistical aggregates. In *IEEE Conference on Computer Vision and Pattern Recognition (CVPR)*. IEEE, 2112–2119.
- [20] Peter Shoubridge, Miro Kraetzl, WAL Wallis, and Horst Bunke. 2002. Detection of abnormal change in a time series of graphs. *Journal of Interconnection Networks* 3, 01n02 (2002), 85–101.
- [21] Robert R Sokal. 1958. A statistical method for evaluating systematic relationships. *Univ Kans Sci Bull* 38 (1958), 1409–1438.
- [22] Pei Sun, Sanjay Chawla, and Bavani Arunasalam. 2006. Mining for outliers in sequential databases. In *Proceedings of the 2006 SIAM International Conference on Data Mining*. SIAM, 94–105.
- [23] Jun Tao, Jian Xu, Chaoli Wang, and Nitesh V Chawla. 2017. HoNVIs: Visualizing and Exploring Higher-Order Networks. *IEEE PacificVis* (2017).
- [24] Christina Warrender, Stephanie Forrest, and Barak Pearlmutter. 1999. Detecting intrusions using system calls: Alternative data models. In *Proceedings of the 1999 IEEE Symposium on Security and Privacy*. IEEE, 133–145.
- [25] Jian Xu, Thanuka L Wickramaratne, and Nitesh V Chawla. 2016. Representing higher-order dependencies in networks. *Science advances* 2, 5 (2016), e1600028.
- [26] Jian Xu, Thanuka L Wickramaratne, Nitesh V Chawla, Erin K Grey, Karsten Steinhäuser, Reuben P Keller, John M Drake, and David M Lodge. 2014. Improving management of aquatic invasions by integrating shipping network, ecological, and environmental data. In *Proceedings of the 20th ACM SIGKDD international conference on Knowledge discovery and data mining*. ACM, 1699–1708.